Stress-Strain Relationship for Nanosilica-Incorporated Lightweight Aggregate Concrete under Compressive Monotonic and Cyclic Loading

H. Dabbagh, K. Babamoradi, K. Amoorezaei

Department of Civil Engineering, University of Kurdistan, Sanandaj, Iran

ABSTRACT: Compared with normal-weight concrete, lightweight aggregate concrete (LWAC) has a lower compressive strength. However, its plus points, including preferable fire resistance, appropriate durability, and dead-load decline lead to the LWAC's application in the construction industry. A practical method to overcome its drawback could be adding nano-silica (NS) to the mixes. For this purpose, the current experimental work aimed at researching to explore the compressive response of LWAC containing different dosages of nano-silica. Therefore, cylindrical specimens of size 150×300 mm improved by nano-silica were subjected to compressive cyclic and monotonic loading; six dosages of NS, including 0, 1, 2, 3, 4, and 5 weight percent of cement were added to mixes as cement replacement. Experimental stress-strain curves were investigated to determine the stress-strain relationships. The results show that the addition of up to 3 wt % nano-silica improves the properties of LWAC, as it was found to enhance compressive strength and modulus of elasticity during monotonic loading, shift up the common point coordinate, and reduce the stiffness degradation of the reloading paths in cyclic loading. However, larger dosages of nano-silica (4% and 5%) were found to have diminishing returns, considering the improved properties of LWAC. Furthermore, stress-strain models for the nano-silica-incorporated LWAC were proposed in compression. The experimental findings were also compared with the proposed model. There was an acceptable concurrence between the proposed model data and experimental findings.

1- Introduction

An appropriate application of computational simulation to understand the actual structural behavior of concrete structures exposed to various loading regimes, in general, and compressive cyclic loading, in particular, is dependent on the existence of accurate stress-strain models predicting critical points on the stress-strain curve. Therefore, to develop an effective model that can predict the hysteretic characteristics of the material in cyclic loading, it is significant to investigate the compressive behavior of concrete. Since the first efforts in this field, fundamental points on the cyclic curve of concrete have been defined; this trend has increased with the evolution of computational methods.

Sinha et al. [1] were one of the first to perform experiments on concrete and to investigate its cyclic compressive curve. A series of cylinders were tested to determine the properties of their unloading, reloading, and envelope curves. An analytical stress-strain relationship was proposed for cyclic loading. It was assumed that the loading history did not affect the envelope, unloading, and reloading curves, which pass through the stress-strain plane. However, Karsan and Jirsa [2], as well as Bahn and Hsu [3], have refuted this assumption.

Karsan and Jirsa [2] performed a study on concrete under compressive loading. According to their results, the upper bound of the cyclic path represents the envelope curve, and the monotonic curve can be used as the envelope curve. Moreover, the plastic strain was of significant importance in formulating the unloading curve, and an equation was established to describe the correlation of the plastic with the envelope unloading strain.

Yankelevsky and Reinhardt [4] used a set of linear curves to show the unloading and reloading paths. Bahn and Hsu [3] studied the key parameters, which control the shape of the cyclic curve in a semi-empirical manner, combining theoretical simulation and experimental test results.

Palermo and Vecchio [5] applied a compression field approach, under compression, to develop their model. They used the Ramberg-Osgood formulation [6] to predict the unloading path. Furthermore, a linear path was accepted as a model for the reloading curve with degrading stiffness in each loading cycle. Moreover, the envelope curve was represented by the monotonic response of the concrete.

Despite the development of various compressive stress-strain models and efforts for predicting the concrete behavior under different loading conditions, a model that can correctly predict the response of nanoparticle-enhanced concrete is still needed.

Recently, some researchers have examined the impact of pozzolanic materials on the mechanical behavior of concrete. In these studies, nano-silica (NS) was found to improve the features of concrete by reducing porosity, increasing

*Corresponding author's email: h.dabbagh@uok.ac.ir

the strength of the hardened cement matrix, and modifying the interfacial transition zone of the aggregate with cement paste [7–10]. Besides, some studies have also explored the beneficial effects of NS on specific characteristics of lightweight aggregate concrete (LWAC) such as compressive behavior [11, 12]; but, no one has developed models to predict the cyclic behavior. Therefore, to understand and improve the characteristics of NS-incorporated LWAC and enhance its potential for use in various applications, this study develops a stress-strain model for NS-incorporated LWAC in uniaxial monotonic and cyclic compressive loading.

2- Experimental work

Details of the experimental work to investigate the influence of NS on LWAC are explained in the following sections.

2. 1. Materials and proportions

Scoria aggregate was used as a fine and coarse lightweight aggregate for preparing the specimens. The largest aggregate size was 12.5 mm, and the 24 h water absorptions of the fine and coarse aggregates were 16% and 12%, respectively. We used ordinary Portland cement (Type I).

The grading of the aggregate was conducted by the ASTM C330 standard [13], and the nano-silica (pozzolanic material) was used in powder form. The Transmission Electron Microscopy (TEM) image of the NS in this study is presented in Fig. 1. To achieve the desired workability, a polycarboxylic-ether-based superplasticizer was added to the mixture. Additional information about the materials is indicated in Table 1.

2.2. Test specimens, mixing, casting, and curing

A volumetric method, ACI 211.2 [14], was used to design the plain LWAC mix. Initially, the fine lightweight aggregate was mixed with the coarse lightweight aggregate. Then, the cement and the water containing NS and superplasticizer were gradually added to the mixer. Six NS-LWAC mixes containing 0, 1, 2, 3, 4, and 5 cement wt% NS were prepared; NS was used as a replacement for cement for the production of concrete mixes. The properties and composition of mixtures in this study are shown in Table 2. These compositions were then cast into the molds and vibrated on a shaking table. Polyethylene sheets were used to cover the specimen surfaces to avoid loss of humidity. After one day, the cylinders were demolded and treated in water over 28 days at 23 ± 2 °C. Before the test, the cylindrical specimens were capped with a sulfur capping compound to obtain a smooth surface so that the load could be transferred uniformly. In this experimental work, at least 36 specimens were tested: 18 cylinders for monotonic testing and 18 cylinders for cyclic testing. No less than three specimens were produced for each mixture.

2.3. Test procedure and setup

Fig. 2 shows a schematic representation of the test setup. To determine the stress-strain curves, a 3000 kN hydraulic compressive testing machine was used to test the specimens. The loading assembly included hydraulic jacks with a 50 mm maximum ram travel, a load spreader, and a bottom plate marked to the center of the cylindrical specimens.

The process detailed in ASTM C469 [15] was applied to investigate the modulus of elasticity, and the process in ASTM C39 [16] was followed to obtain the compressive strength. To

Table 1. Material properties

Materials	Type	Specific density [kg/m^3]
Cement	Ordinary Portland (Type I)	3150
Fine lightweight aggregate	Scoria	Bulk density: 772 Apparent specific gravity: 1650
Coarse lightweight aggregate	Scoria	Bulk density: 680 Apparent specific gravity: 1530
Superplasticizer	Polycarboxylic ether	1080
Pozzolanic material	Nanosilica (NS)	50

Table 2. Mix proportions

Samples	C [kg/m^3]	CA [kg/m^3]	FA [kg/m^3]	W/(C+NS) Ratio	SP [kg/m^3]	NS [kg/m^3]
Ref	460	528	584	0.31	2.4	0
N1	455.4	528	584	0.31	2.6	4.6
N2	450.8	528	584	0.31	2.7	9.2
N3	446.2	528	584	0.31	2.8	13.8
N4	441.6	528	584	0.31	2.9	18.4
N5	437	528	584	0.31	3.0	23

C: Cement, CA: Coarse aggregates, FA: Fine aggregates, W: Water, SP: Superplasticizer, NS: Nanosilica
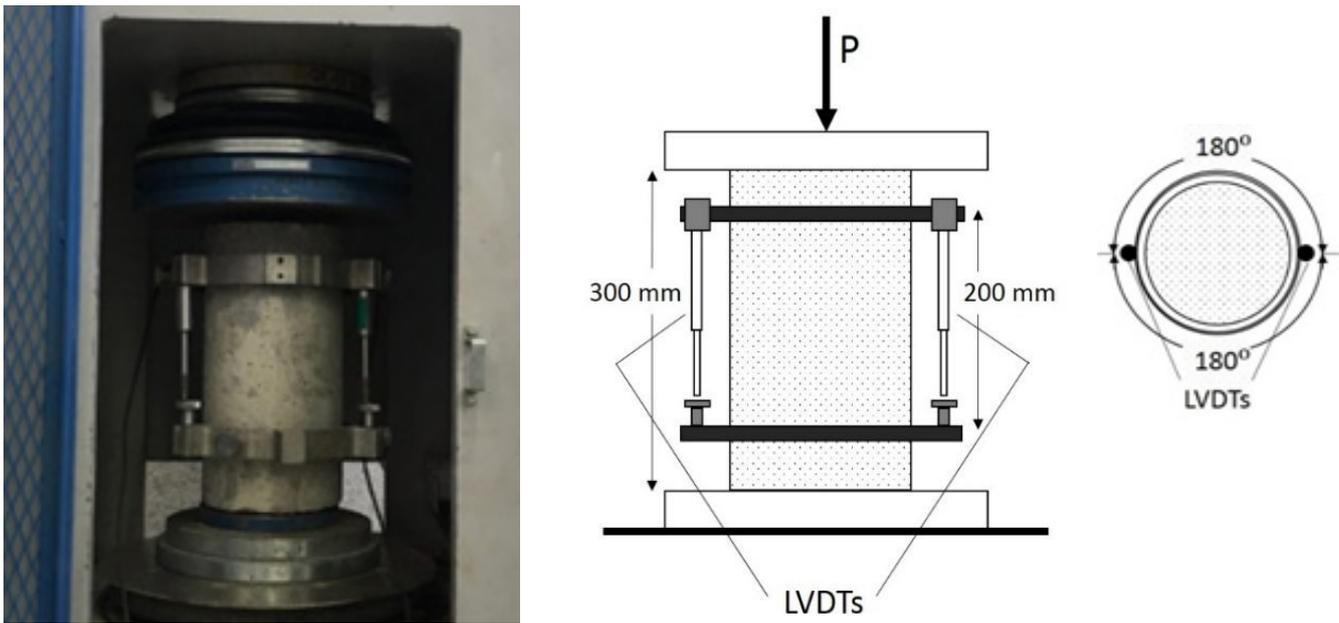
Fig. 2. Test setup for generating the stress-strain curves of the NS-incorporated LWAC
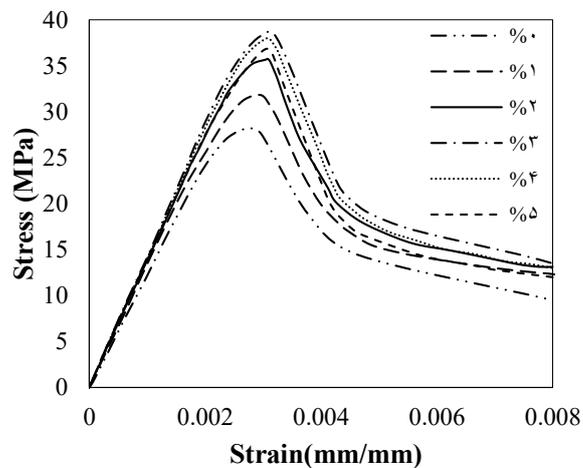
Figure 3. Monotonic stress-strain curve of the NS-incorporated LWAC

obtain the stress-strain curves, two linear variable differential transducers (LVDTs), which were parallel to the specimens (Fig. 2), were used to measure the displacement, and a circular steel frame was built to grip the LVDTs. The axial deformation of the cylinders was measured by the LVDTs, and a data logger was used to record the data. The output from the data logger was averaged for more precise results. As the loading progressed, the uniaxial load was maintained concentric to the cylindrical specimen.

In the current study, the cyclic loading pattern of complete unloading and reloading cycles to the envelope curve was employed, meaning that unloading began from the envelope curve to the zero stress level, and the reloading began from the end of the previous unloading curve to the envelope. Regarding the cyclic load history, four cycles of unloading and reloading were imposed, one cycle before the peak stress and three cycles beyond the maximum stress. To accurately recognize the impact of NS on the key parameters defining

the stress-strain curve, the unloading started at the same value of unloading strain, for each cycle, in various stress-strain curves.

The loading process provided the concrete cyclic and monotonic stress-strain curves.

3- Experimental results
3.1. Monotonic loading

To obtain the stress-strain curve, compressive monotonic loading conditions were applied to the cylindrical specimens. The main parameters were investigated, and the effect of NS on these parameters was recognized.

The addition of NS influences both the descending and ascending branches of the curve (Fig. 3). Adding 1% NS (N1) enhances the slope of the ascending branch and the modulus of elasticity (E). At the descending branch for the N1 mix, the rate of decrease of the strength is faster, and the descending branch slope is different from that of the reference curve. Furthermore, the addition of 2% NS improves the properties of the Ref sample. For the mix containing 3% NS (N3), the ascending branch considerably improves, and a significant enhancement is also observed in both compressive strength (f_c) and modulus of elasticity. Moreover, the samples are brittle compared to the reference, N1, and N2 mixes. However, a larger dosage of NS (4%) has a little negative effect, considering the improved properties of LWAC. For the 5% NS (N5) mix, the slope of the ascending branch is lower in comparison to the N3 and N4 mixes. A steeper drop in strength occurs after maximum stress, and the sample shows more brittleness than the other mixes. Based on this investigation, 3% NS was determined to be the best dosage for improving the features of lightweight concrete.

When hydration is in progress, a layer is produced on the cement grain surface owing to the hydration. For a hardened plain sample, the porosity is high, and the compressive strength is relatively low. By adding NS to the mixture, calcium silicate hydrate (C-S-H) seeds are produced on the NS surface (a positive effect). The pozzolanic reaction of silica with portlandite (Ca(OH)$_2$), which is formed during the ordinary Portland cement hydration leads to the production of additional calcium silicate hydrate (C–S– H) on the NS surface which is the prime cause of strength and density in the hardened cement paste. Simultaneously, (Ca(OH)$_2$), which hardly plays a role in improving strength, is consumed. In other words, the reaction of NS particles with aqueous calcium ions released by cement dissolution constitutes C-S-H on their surface [17, 18]. Therefore, the C-S-H gel will be produced on both the grain and silica surfaces.

The use of small amounts of NS (less than 2%) leads to the generation of small quantities of new C-S-H seeds, while hydration occurred on the remaining cement surface. This is an indication that a large number of pores exist in the hardened cement matrix. A high concentration of NS (e.g., 5%) produces a thick C-S-H layer on the silica surface that greatly increases the viscosity of the mixes.

The addition of NS to the mixture significantly increases the amount of entrapped air in the cementitious system (a negative effect). When the NS concentration is optimal (3%), a balance is maintained between the positive and negative influences of NS on the properties of concrete, and the compressive strength increases considerably. This phenomenon has been reported in the literature [19].

Table 3 presents the compressive strength of LWAC containing various weight fractions of NS. The compressive strength is 28.2 MPa for the plain concrete, and the values are 31.7, 35.7, 38.5, 38, and 36.8 MPa for the concrete mixes containing 1, 2, 3, 4, and 5 wt% NS, respectively. Compared to plain concrete, the compressive strength improves by 12.4%, 26.6%, 36.5%, 34.7%, and 30.5% for the samples with NS additions of 1, 2, 3, 4, and 5 wt%, respectively.

The moduli of elasticity are 12.18, 13.14, 13.95, 14.45, 14.39, and 14.13 GPa for samples with 0, 1, 2, 3, 4, and 5 wt% NS, respectively, as presented in Table 3. Based on these findings, NS addition has a considerable impact on the E; it improves by 8%, 14.5%, 18.6%, 18.1%, and 16% for specimens containing 1, 2, 3, 4, and 5 wt% NS, respectively.

According to the experimental findings, the following equations can be derived for the NS-incorporated LWAC (Figs. 4, 5, and 6)

Table 2. Mix proportions

Samples	f_c [MPa]	E [GPa]	ε_0 [mm/mm]
Ref	28.2	12.18	0.00274
N1	31.7	13.14	0.00297
N2	35.7	13.95	0.00305
N3	38.5	14.45	0.00318
N4	38	14.39	0.00314
N5	36.8	14.13	0.00306
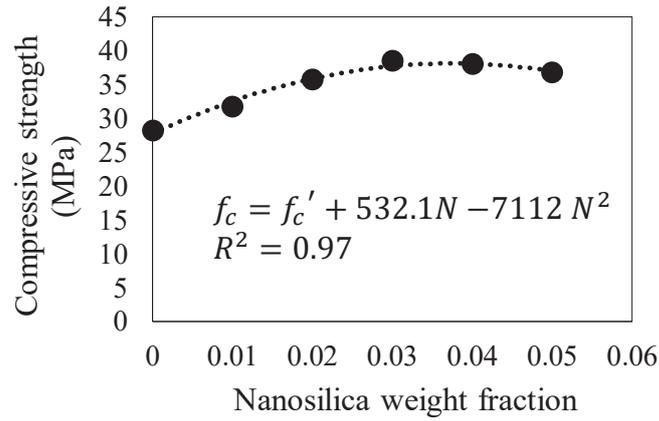
Fig. 4. Relationship between f_c **and** N

$$f_c = f_c{}' + 532.1N - 7112\,N^2$$
$$R^2 = 0.97$$
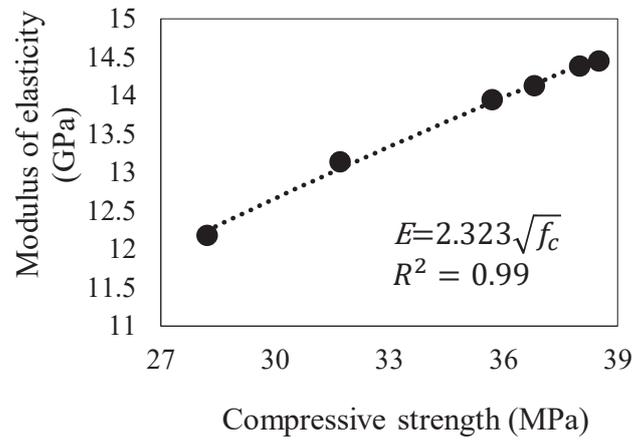
Fig. 5. Relationship between E **and** f_c
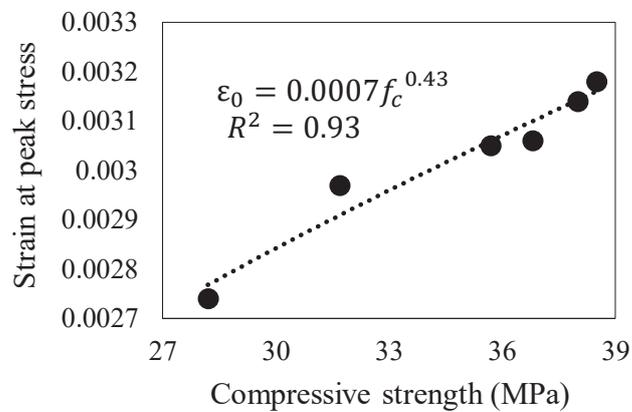
$$E = 2.323\sqrt{f_c}$$
$$R^2 = 0.99$$

Fig. 6. Relationship between ε_0 **and** f_c
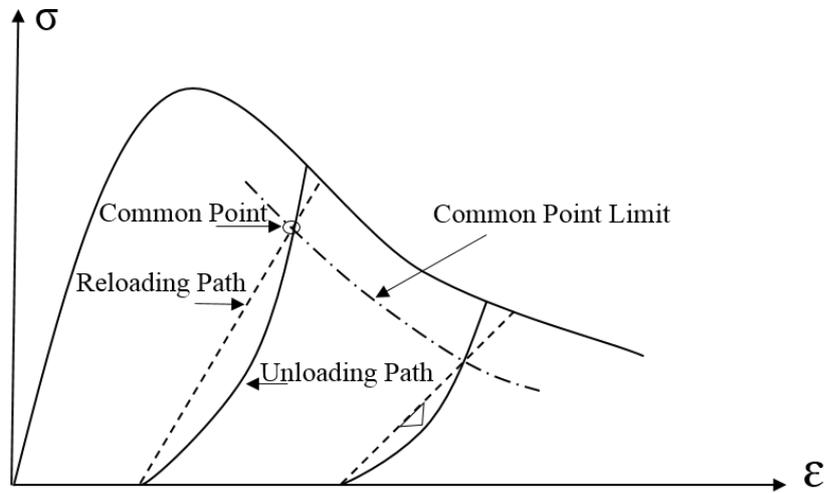
$$\varepsilon_0 = 0.0007 f_c{}^{0.43}$$
$$R^2 = 0.93$$

Fig. 7. Schematic diagram highlighting the key features of a cyclic stress-strain curve

$$f_c = f_c' + 532.1N - 7112N^2 \qquad R^2 = 0.97 \qquad (1)$$

$$E = 2.323\sqrt{f_c} \qquad R^2 = 0.99 \qquad (2)$$

$$\varepsilon_0 = 0.0007 f_c^{0.43} \qquad R^2 = 0.93 \qquad (3)$$

where f_c denotes the compressive strength of NS-incorporated LWAC in MPa, f_c' refers to the compressive strength of plain lightweight concrete in MPa, E denotes the modulus of elasticity in GPa, ε_0 represents the strain at peak stress in mm/mm, and N is the NS weight fraction.

3. 2. Cyclic loading

Experimental tests were performed to analyze the effects of NS on LWAC behaviors in cyclic compression. The significant parameters in the cyclic stress-strain path, as well as the failure modes, were investigated. Fig. 7 shows a schematic representation of the key parameters determined from a cyclic stress-strain curve.

3. 2. 1. Stress-strain curve

Fig. 8 illustrates the results of the cyclic experimental tests. Based on the results, all the parameters that influence the cyclic curve are functions of the point of unloading. Moreover, the monotonic curve can almost describe the upper bounds of the cyclic curve, although there is a slight

difference between them, which is caused by the damage due to reloading and unloading cycles.

After the maximum stress, the stress-strain curve sharply decreases. The aggregates in LWAC are the weakest constituent of the cement matrix as compared to normal-weight concrete where the hardened paste is the weakest. Consequently, the cutback in the post-peak stress is more apparent in comparison with normal-weight concrete, particularly in cyclic loading [20].

3. 2. 2. Common point

One of the key parameters in a cyclic curve is the "common point" (CP), which is defined as the point of intersection between the reloading and unloading curves; its value determines the "CP limit". At the CP limit, the reloading path changes noticeably. In previous studies, it has been shown that changes in the slope of the reloading curve after the CP can be due to a significant increase in microcracking [21].

The stress above the CP limit results in additional strains, whereas stress at or below this limit leads to the creation of stress-strain loops [22]. As presented in Fig. 9(a) upon addition of up to 3% NS, the coordinate of the CP moves up, and a higher CP limit is obtained. However, adding large amounts of NS (4% and 5%) shifts the coordinates of CP downwards in comparison to the addition of 3% NS. The changes in the position of the CP upon the addition of NS are the result of changes in the bearable stress level of samples with different dosages of NS.
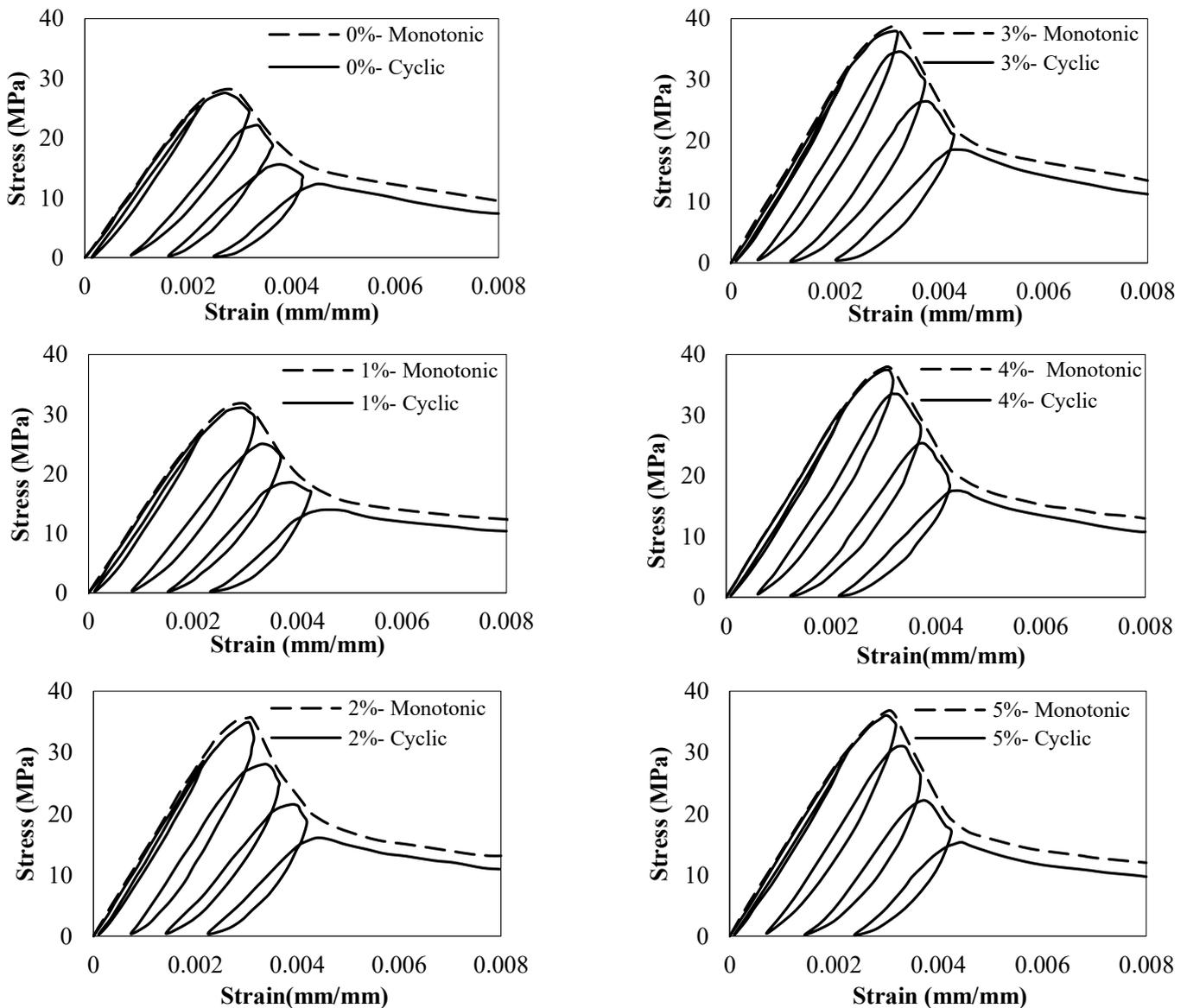
Fig. 8. Cyclic stress-strain curve of the NS-incorporated LWAC

3.2.3. Unloading and reloading path

If the strain from the value above the elastic limit of the material decreases, an "unloading curve" is formed. Furthermore, a set of unloading curves can be obtained by changing the unloading strain. In the complete cyclic loading regime, after unloading, the strain rises again from the zero-stress level (or near-zero stress level). The "reloading curve" is the path that starts from the final point on the unloading curve and ends at the envelope curve. Moreover, the reloading curves that begin from different strains are called the "set of reloading curves".

According to the experimental results (Fig. 8), the unloading and reloading paths for the NS-incorporated LWAC are nonlinear. Some researchers have assumed a linear path for the reloading curves. However, to achieve a perfect simulation of concrete behavior, the nonlinear response of concrete beyond the CP should be considered.
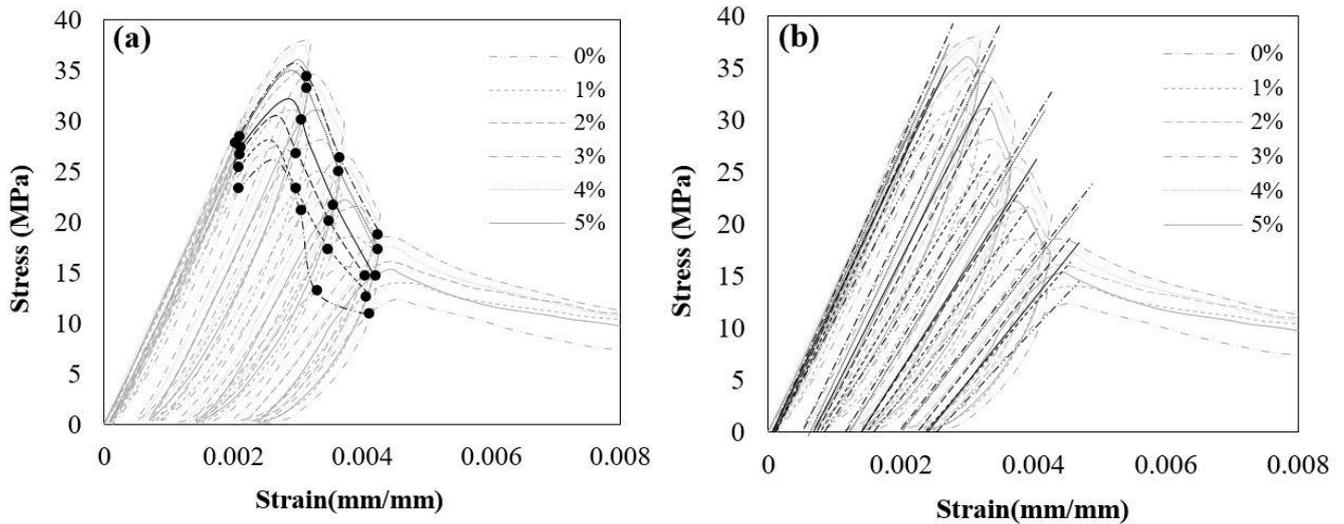
Fig. 9. Effect of the added NS on the (a) common point limit and (b) stiffness

3.2.4. Reloading strength and tangent

Reloading strength refers to the maximum stress tolerated by damaged concrete upon reloading [22]. The value of reloading stress depends on the dosage of NS. Increasing the amount of NS to 3% improves the reloading strength, whereas the improvement for the N4 and N5 mixes is less than that for N3.

In Fig. 9(b), the reloading paths of the stress-strain curve are not parallel to the initial loading path. Moreover, the slope of the reloading curve from the zero-stress level (reloading tangent) decreases in each cycle. The decrease in the slope indicates a degradation of the stiffness due to crack expansion during cyclic loading throughout the entire strain range. The cyclic curve of the N3 mix showed the least degradation in stiffness, as compared to the other mixes. The effect of NS on the production of silica gel may result in changes in the reloading tangent and strength.

3. 3. Failure mode

At the peak load level, the lateral expansion of the concrete results in deep cracks in the specimens. Cylindrical specimens containing different weight fractions of NS were subjected to two regimes of compressive loading: cyclic and monotonic. Fig. 10 shows the specimens after testing. It is clear that the failure modes are nearly similar under the monotonic and cyclic regimes. The considerable difference between cylinders exposed to different loadings (cyclic and monotonic) is related to the depth of the cracks.

In the Ref sample, cracks propagate parallel to the loading direction. According to Fig. 10, NS addition does not change the failure mode, and the cracks are nearly parallel to the loading direction, similar to the plain concrete, for both the monotonic and cyclic tests. However, adding large amounts of NS (4% and 5%) results in deeper cracks in comparison with the other specimens.

4- Proposed equations (stress-strain relationships)

The monotonic and cyclic responses of the NS-incorporated LWAC can be predicted by equations that define the characteristics of the curve. Mathematical expressions are established to predict the plastic strain, reloading strain, envelope curve, monotonic curve, as well as unloading and reloading curves. According to the experimental data, the optimal dosage of NS is 3% by weight of cement. Adding NS up to 3% improves the characteristics of the lightweight concrete, whereas using more than 3% NS deteriorates the improvement in the characteristics. Therefore, stress-strain relationships are established based on a maximum of 3% NS.

In this section, the normalized coordinates, $U = \sigma/f_c$ and $S = \varepsilon/\varepsilon_0$ are used for stress and strain, respectively, for better comparison. U represents the stress ratio, and S denotes the strain ratio. The stress coordinate σ is normalized relative to f_c, the 28-day cylindrical strength, and the strain coordinate ε is normalized relative to ε_0 the strain at peak stress. Each curve is normalized by its own f_c and ε_0 values.

4. 1. Monotonic curve

For concrete under compression, the following conditions are used to propose an equation for the stress-strain curve [23]:

1. The equations should be comparable with all experimental results.
2. The complete stress-strain curve, including the descending and ascending parts, should be described.
3. The equations should be as simple as possible.
4. The proposed equations should be based on essential parameters, f_c, ε_0, and E, as described earlier. These parameters can be determined by experimental data. At the point of origin, $\sigma = 0$, and at the point of peak stress,

$$d(\sigma)/d(\varepsilon) = 0.$$

(a). N= 0%

(b). N= 1%

(g). N= 0%

(h). N= 1%

(c). N= 2%

(d). N= 3%

(i). N= 2%

(j). N= 3%

(e). N= 4%

(f). N= 5%

(k). N= 4%

(l). N= 5%

Fig. 10. Failure mode of NS-incorporated LWAC under (a–f) monotonic and (g–l) cyclic compressive loading

Many stress-strain models were studied, and the equation introduced by Popovic [24] was modified to predict the monotonic curve. The empirical equation for the monotonic curve of NS-incorporated LWAC (maximum of 3 wt% NS) can be expressed as follows:

$$\frac{\sigma}{f_c} = \frac{\beta\left(\dfrac{\varepsilon}{\varepsilon_0}\right)}{\beta - 1 + \left(\dfrac{\varepsilon}{\varepsilon_0}\right)^{\alpha}} \tag{4}$$

$$\alpha = \beta = 6\exp\left(-1.7N\right)\alpha = 1.6 + 9N \quad \varepsilon \le \varepsilon_0 \tag{5}$$

$$\alpha = 1.6 + 9N \qquad \varepsilon > \varepsilon_0 \tag{6}$$

$$\beta = 0.6 + 4N \qquad \varepsilon > \varepsilon_0 \tag{7}$$

where ε and σ denote the strain and stress on the curve, respectively, and α and β are parameters dependent on the stress-strain curve shape. All these parameters are functions of the weight fraction of NS (N), so N is necessary for plotting the curve.

4. 2. Envelope curve

The locus of points that connect the end of the reloading curves and the beginning of the unloading curves is called an "envelope curve." Based on the experimental results, cyclic stress-strain paths do not exceed the envelope curve. The envelope curve of a compressive cyclic loading curve can be approximated by the monotonic path [3]. However, Fig. 8 demonstrates the differences between the envelope curve and the monotonic stress-strain path. This dissimilarity at the beginning of compressive loading is negligible; nevertheless, it becomes more apparent by applying more cycles of unloading and reloading.

At a specific strain, the envelope curve shows a sharp decline, whereas the monotonic curve gradually falls. Therefore, the difference that was negligible at the beginning approaches nearly 10% by the end of the strain range. In this work, based on the Popovic model [24], a separate model is proposed for the envelope curve to better reflect the experimental findings.

$$U_{eu} = \frac{\gamma\left(S_{eu}\right)}{\gamma - 1 + \left(S_{eu}\right)^{\lambda}} \tag{8}$$

$$\lambda = \gamma = 6\exp\left(-1.7N\right) \qquad \varepsilon \le \varepsilon_0 \tag{9}$$

$$\lambda = 1.85 + 10N \qquad \varepsilon > \varepsilon_0 \tag{10}$$

$$\gamma = 0.63 + 4N \qquad \varepsilon > \varepsilon_0 \tag{11}$$

where U_{eu} and S_{eu} denote the stress and strain ratios on the envelope curve, respectively, and λ and γ are material parameters.

4. 3. Plastic strain

The shape of the stress-strain path will be modified when the plastic strain changes. Therefore, an equation describing the association between the unloading and plastic strain ratios on the envelope curve would be useful. An analytical expression of the plastic strain ratio has been proposed by Bahn and Hsu [3], which agrees well with the experimental test findings. Eq. (12) is a modified form of their model, showing the NS impact on the compressive behavior of lightweight concrete. To define the association of plastic strain with envelope unloading strain ratios, the following equation is proposed. In Fig. 11, the model proposed herein is compared with the experimental data.

$$S_p = C_f\left(S_{eu}\right)^{n_f} \tag{12}$$

$$n_f = 8.4N + 3.75 \tag{13}$$

$$C_f = 0.2 \tag{14}$$

where S_p represents the plastic strain ratio, S_{eu} denotes the envelope unloading strain ratio (refers to the strain ratio on the envelope curve in Section 4.2), C_f is the coefficient of plastic strain, and n_f is the order according to the experimental data. Based on the present experimental study, the constant coefficient, C_f, is 0.2 and for n_f, a polynomial term in the form of Eq. (13) is defined.

4.4. Reloading strain

The reloading strain corresponds to the strain observed at the end of the reloading path for each cycle. As it is located on the envelope curve, the reloading strain can also be called the "envelope reloading strain."

The relationship of the envelope reloading strain ratio with the envelope unloading strain ratio is presented in Fig. 12. The following equation is obtained based on the experimental findings:

$$S_{er} = \left(1.07 - N\right)S_{eu}^{1.09} \tag{15}$$

where S_{er} denotes the envelope reloading strain ratio.

It is difficult to pinpoint the exact location of the reloading strain on the experimental envelope curve. Therefore, the published relationship between the envelope reloading and unloading strain ratio is an approximate equation.
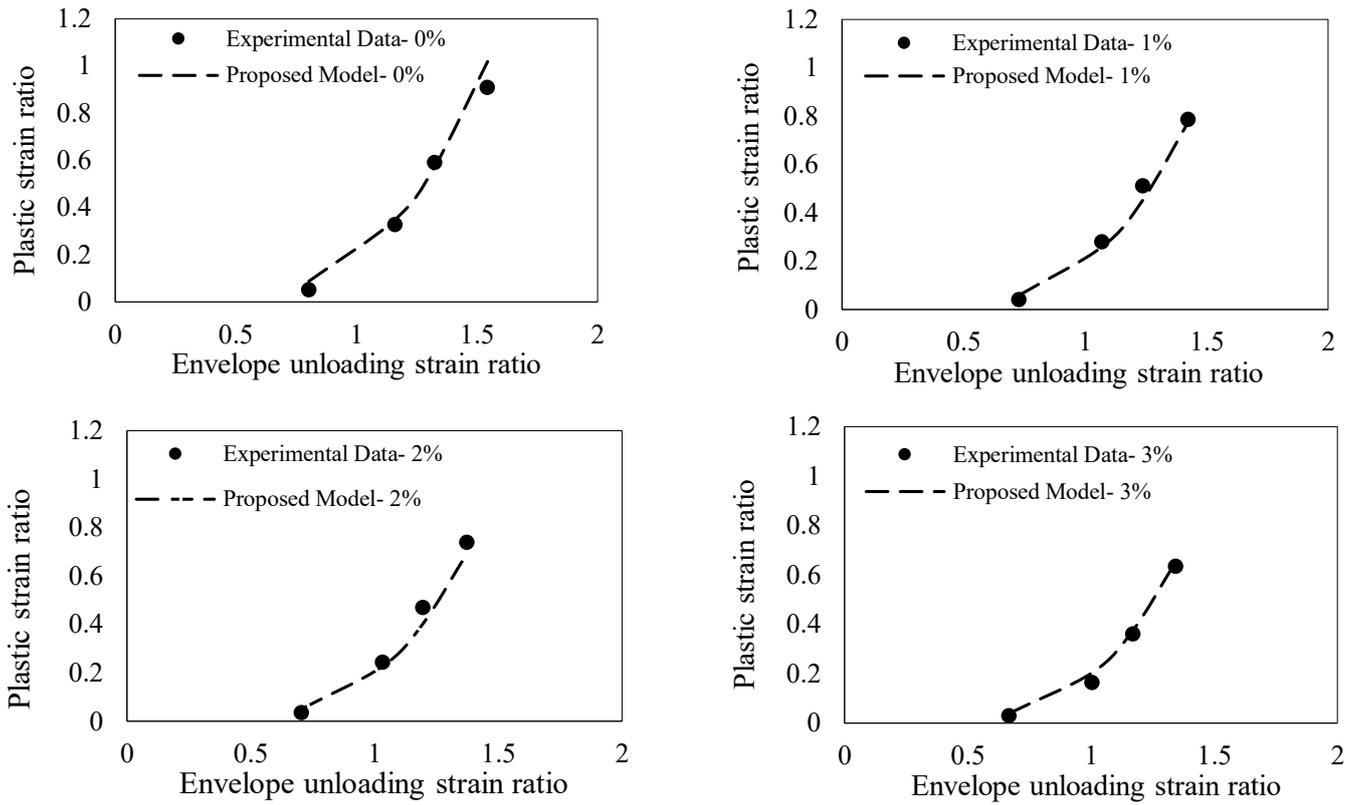
Fig. 11. Relationship between S_p and S_{eu}

4.5. Unloading and reloading curve

Along with the strain range in the stress-strain plane, the degree of nonlinearity, also called the curvature, varies for the unloading path. Therefore, the term that defines the order of the expression proposed for the unloading path should be a function of the plastic strain ratio. Moreover, the dependence of the plastic strain ratio on the dosage of NS should be considered. The proposed mathematical equation is written as follows to predict the unloading path:

$$U_{unlo} = U_{eu}\left(\frac{S - S_p}{S_{eu} - S_p}\right)^{n_p} \tag{16}$$

$$n_p = a + b\sqrt{S_p} \tag{17}$$

$$a = 2.2N + 0.9 \tag{18}$$

$$b = 14.7N + 1.2 \tag{19}$$

U_{unlo} is the unloading stress ratio, U_{eu} is the envelope unloading stress ratio (refers to the envelope curve stress ratio as defined in Section 4.2), and n_p is a function of the

plastic strain. If n_p is assumed to be 1.0, the proposed model will be linear, which joins the unloading point to the plastic strain on the zero-stress level at the end of the unloading path. The stress-strain relationship proposed for the unloading curves considers the properties of unloading paths from the experimental tests, including the initial and final stiffness values and the curvature of the paths.

Fig. 8 illustrates that the shape of the reloading paths is a function of the plastic strain ratio. Therefore, the plastic strain is considered a variable in forming the reloading path. The stress-strain path for reloading curve of NS-incorporated LWAC can be determined as follows:

$$U_{relo} = C_u \times U_{eu}\left(1 - c\left(\frac{S}{S_p}\right)^{m_p}\right)\left(\frac{S - S_p}{S_{eu} - S_p}\right) \tag{20}$$

$$c = d + e\left(S_p\right) \tag{21}$$

$$d = -0.065N - 0.014 \tag{22}$$
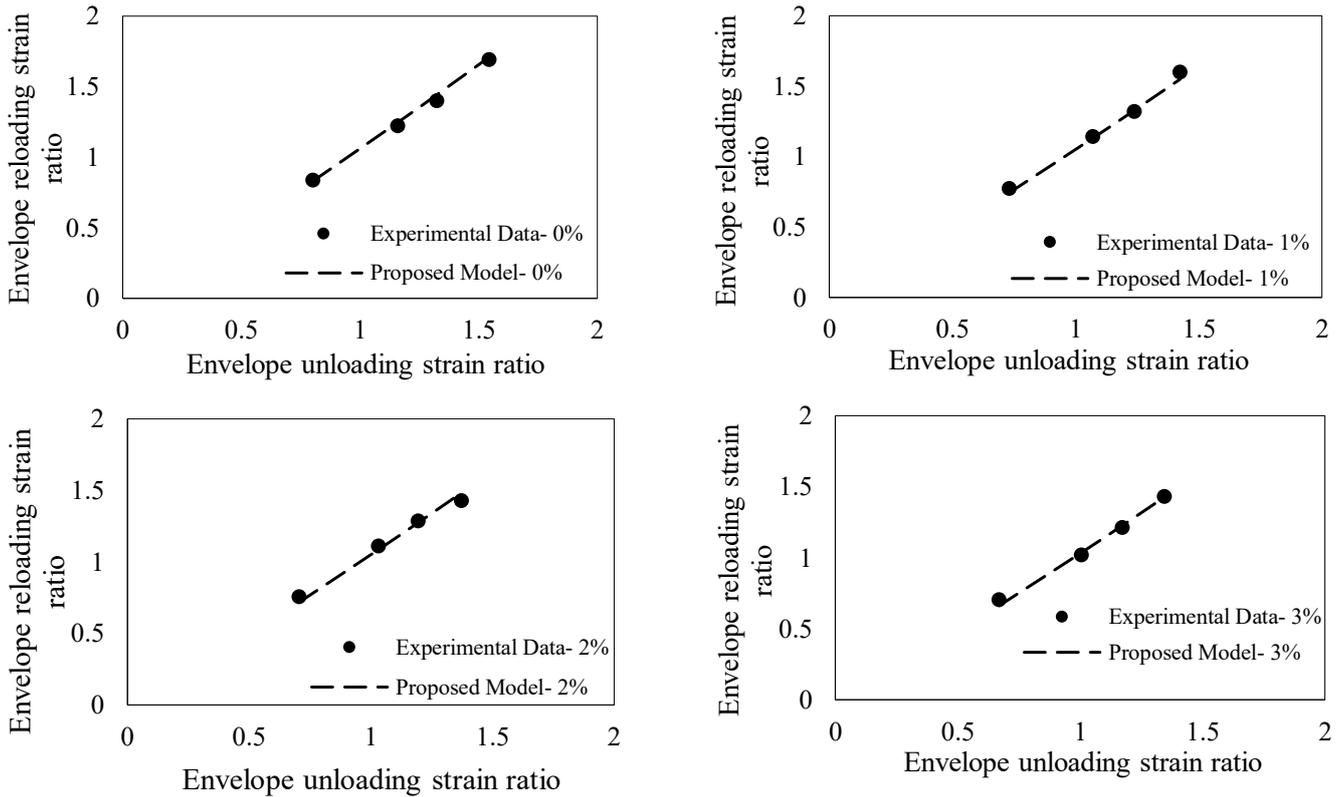
Fig. 12. Relationship between S_{er} **and** S_{eu}

$$e = 0.405N + 0.092 \qquad (23)$$

$$m_p = 0.1 \qquad C_u = 0.97 \qquad S \leq 1 \qquad (24)$$

$$m_p = 1.8 \qquad C_u = 1 \qquad S > 1 \qquad (25)$$

where U_{relo} represents the reloading stress ratio and C_u is a parameter of the reloading curve. C_u is a variable, while according to the experimental data, the best values are 0.97 and 1, respectively, considering the S value. The presented equation for the reloading curve passes through three points, including the point at which the reloading curve begins, the CP, and the point where the curve approaches the envelope curve.

There is a noticeable advantage to the reloading curve of the proposed model compared to models reported previously in the literature. This model does not depend on the reloading strain on the envelope curve, which is normally an assumed value. Furthermore, the model can easily describe the initial modulus of elasticity for each reloading curve, whereas most models have been constructed based on the assumption of a linear reloading path and cannot trace the exact experimental path.

5- Fit of the proposed model to the experimental test data

A comparison was conducted, and the established stress-strain model was validated. The stress-strain relationship predicts the behavior of NS-incorporated LWAC up to 3 wt% NS. Therefore, the comparison is conducted for samples with 0, 1, 2, and 3% NS. Figs. 13(a–h) illustrate the monotonic and cyclic curves of NS-incorporated LWAC determined from the proposed model and the experimental tests. The predicted and experimental data matched well at the different NS weight fractions. The proposed model clearly shows the considerable effects of NS on the ascending branch of the monotonic curve, f_c, and E. Furthermore, it shows a decrease in strength beyond the peak stress (Figs. 13(a-d)).

The experimental results have been used to recognize the ability of the model to estimate the unloading and reloading paths (Figs. 13(e-h)). The stress-strain relationship provides a good fit with the experimental unloading and reloading paths for different dosages of NS (up to 3 wt%). The stiffness degradation of NS-incorporated LWAC after each cycle of unloading and reloading is reflected by the lower slope of the reloading path. Furthermore, the model predicts softening in the response of the concrete beyond the CP. Proposing a model for the envelope curve distinguished from the monotonic curve results in a satisfactory simulation of the upper bounds for the cyclic curve.
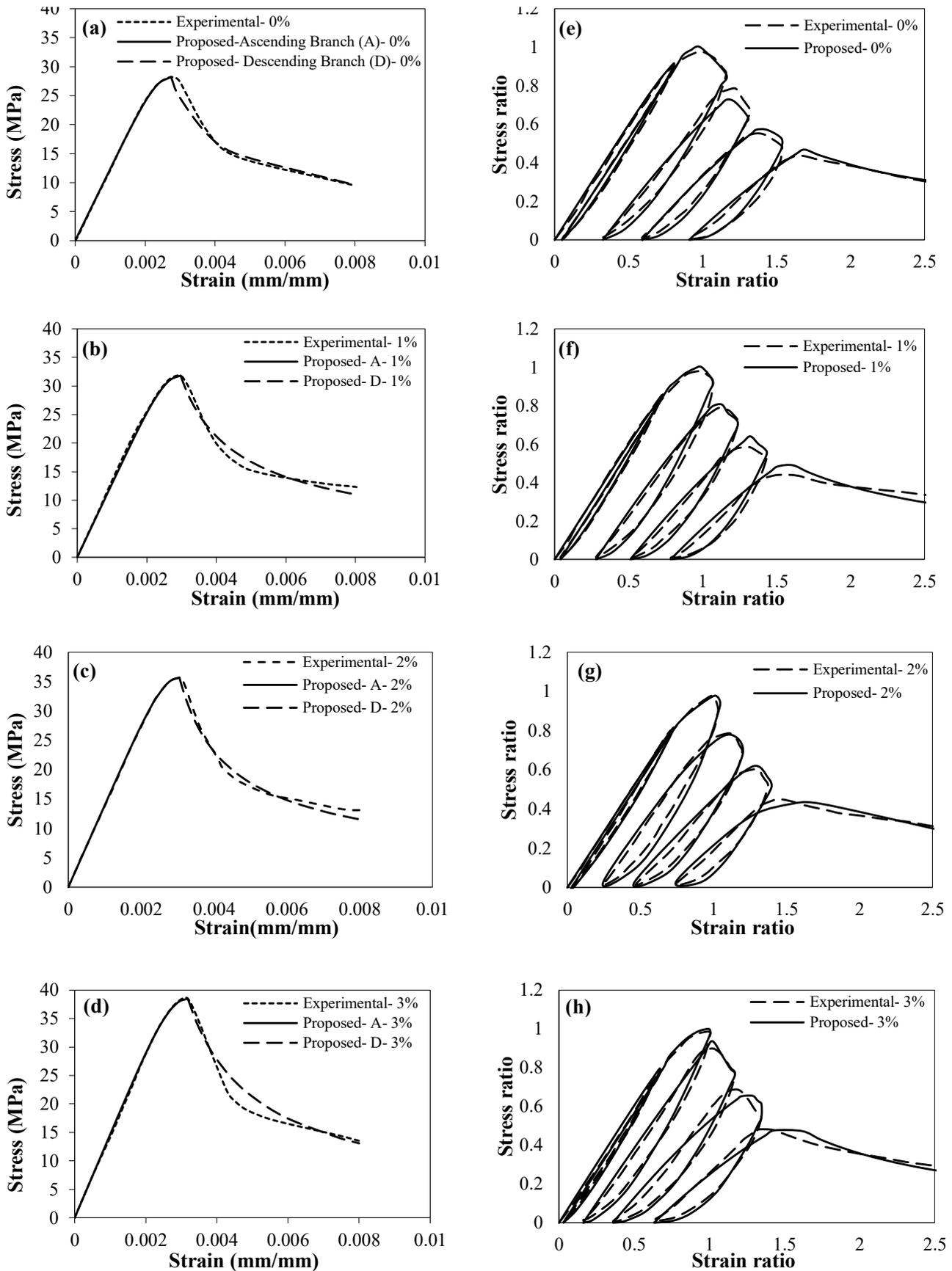
Fig. 13. Fit of the proposed model to the experimental test data- monotonic (a-d) and cyclic (e-h) loading

It should be noted that the lack of investigation in the field of NS-incorporated LWAC subjected to cyclic loading provides a limitation to make a comparison between the proposed model and the experimental work linked to other researchers.

6- Conclusions

Different doses of NS were added to the concrete mixtures to determine the stress-strain relationship for NS-incorporated LWAC, and the influence of NS on the responses of the LWAC to monotonic and cyclic compression was investigated and modeled.

1- The addition of NS (up to 3%) improves the pre-peak monotonic properties of LWAC by increasing the modulus of elasticity and compressive strength. The descending part of the stress-strain path becomes steeper, and the LWAC behaves in a more brittle manner beyond the peak stress. Excessive NS (5%) has a negative influence on the above-mentioned parameters.

2- Adding NS (up to 3%) to the samples subjected to cyclic loading results in a shifting CP limit and reducing the stiffness degradation of consecutive loops.

3- Stress-strain models were proposed for predicting the cyclic and monotonic responses of NS-incorporated LWAC. Nonlinear equations model both the unloading and reloading curves. Furthermore, the upper bounds of the cyclic stress-strain curves are simulated by a model distinct from the previously proposed monotonic loading model. The comparative study reveals satisfactory agreement of the proposed monotonic and cyclic curves with the experimental data.

4- Regression analysis helped establish the relationships of compressive strength, modulus of elasticity, and strain at peak stress with respect to the NS weight fraction. Overall, the proposed equations for modeling plastic and reloading strain ratios reveal a good agreement.

Acknowledgments

Notation

f_c	Compressive strength of nanosilica-incorporated lightweight aggregate concrete
f_c'	Compressive strength of plain lightweight aggregate concrete
σ	Stress on the monotonic curve
ε_0	Strain at peak stress
ε	Strain on the monotonic curve
E	Modulus of elasticity
α	Parameter of monotonic curve
β	Parameter of monotonic curve
N	Nanosilica weight fraction
U	Stress ratio
U_{unlo}	Unloading stress ratio
U_{relo}	Reloading stress ratio
U_{eu}	Unloading stress ratio on the envelope curve
S	Strain ratio
S_{eu}	Unloading strain ratio on the envelope curve
S_{er}	Reloading strain ratio on the envelope curve
S_p	Plastic strain ratio
λ	Parameter of envelope curve
γ	Parameter of envelope curve
C_f	Coefficient of plastic strain
n_f	Parameter of plastic strain
n_p	Parameters of unloading curve
C_u	Parameter of reloading curve

References

[1] B. Sinha, K. H. Gerstle, L. G. Tulin, Stress-strain relations for concrete under cyclic loading, in: Journal Proceedings, (1964) 195-212.

[2] I.D. Karsan, J. O. Jirsa, Behavior of concrete under compressive loadings, Journal of the Structural Division, (1969).

[3] B. Y. Bahn, C. T. T. Hsu, Stress-strain behavior of concrete under cyclic loading, ACI Materials Journal, 95 (1998) 178-193.

[4] D. Z. Yankelevsky, H. W. Reinhardt, Model for cyclic compressive behavior of concrete, Journal of Structural Engineering, 113(2) (1987) 228-240.

[5] D. Palermo, F. J. Vecchio, Compression field modeling of reinforced concrete subjected to reversed loading: formulation, Structural Journal, 100(5) (2003) 616-625.

[6] W. Ramberg, W. R. Osgood, Description of stress-strain curves by three parameters, (1943).

[7] Z. Rong, W. Sun, H. Xiao, G. Jiang, Effects of nano-SiO2 particles on the mechanical and microstructural properties of ultra-high performance cementitious composites, Cement and Concrete Composites, 56 (2015) 25-31.

[8] S. Kawashima, P. Hou, D. J. Corr, S. P. Shah, Modification of cement-based materials with nanoparticles, Cement and Concrete Composites, 36 (2013) 8-15.

[9] L. Singh, D. Ali, U. Sharma, Studies on optimization of silica nanoparticles dosage in cementitious system, Cement and Concrete Composites, 70 (2016) 60-68.

[10] J. Xu, B. Wang, J. Zuo, Modification effects of nanosilica on the interfacial transition zone in concrete: A multiscale approach, Cement and Concrete Composites, 81 (2017) 1-10.

[11] Y. Gao, C. Zou, Experimental study on segregation resistance of nanoSiO2 fly ash lightweight aggregate concrete, Construction and Building Materials, 93 (2015) 64-69.

[12] H. Du, D. Suhuan, L. Xuemei, Effect of nano-silica on the mechanical and transport properties of lightweight

concrete, Construction and Building Materials, 82 (2015) 114-122.

[13] A. Standard, ASTM C330, Standard Specification for Lightweight Aggregates for Structural Concrete, ASTM International, (2014).

[14] J. R. Prestera, M. Boyle, D. A. Crocker, S.B. Chairman, E.A. Abdun-Nur, S.G. Barton, L.W. Bell, G.R. Berg, S.J. Blas Jr, P.M. Carrasquillo, Standard Practice for Selecting Proportions for Structural Lightweight Concrete (ACI 211.2-98), (1998).

[15] A. Standard, ASTM C469, Standard Test Method for Static Modulus of Elasticity and Poisson's Ratio of Concrete in Compression, ASTM International, (2010).

[16] A. Standard, ASTM C39, Standard test method for compressive strength of cylindrical concrete specimens, ASTM International, (2012).

[17] J.J. Thomas, H.M. Jennings, J.J. Chen, Influence of nucleation seeding on the hydration mechanisms of tricalcium silicate and cement, The Journal of Physical Chemistry C, 113(11) (2009) 4327-4334.

[18] G. Land, D. Stephan, The influence of nano-silica on the hydration of ordinary Portland cement, Journal of Materials Science, 47(2) (2012) 1011-1017.

[19] R. Yu, P. Spiesz, H. Brouwers, Effect of nano-silica on the hydration and microstructure development of Ultra-High Performance Concrete (UHPC) with a low binder amount, Construction and Building Materials, 65 (2014) 140-150.

[20] M. H. Zhang, O.E. Gjvorv, Mechanical properties of high-strength lightweight concrete, Materials Journal, 88(3) (1991) 240-247.

[21] G. M. Sturman, S.P. Shah, G. Winter, Microcracking and inelastic behavior of concrete, Special Publication, 12 (1965) 473-499.

[22] S. Sinaie, A. Heidarpour, X.-L. Zhao, J.G. Sanjayan, Effect of size on the response of cylindrical concrete samples under cyclic loading, Construction and Building Materials, 84 (2015) 399-408.

[23] D. J. Carreira, K.-H. Chu, Stress-strain relationship for plain concrete in compression, in: Journal Proceedings, (1985) 797-804.

[24] S. Popovics, A numerical approach to the complete stress-strain curve of concrete, Cement and concrete research, 3(5) (1973) 583-599.